AIP | Applied Physics Letters

Multiple percolation tunneling staircase in metal-semiconductor nanoparticle composites

Rupam Mukherjee, Zhi-Feng Huang, and Boris Nadgorny

Citation: Applied Physics Letters **105**, 173104 (2014); doi: 10.1063/1.4900777
View online: http://dx.doi.org/10.1063/1.4900777
View Table of Contents: http://scitation.aip.org/content/aip/journal/apl/105/17?ver=pdfcov
Published by the AIP Publishing

Multiple percolation tunneling staircase in metal-semiconductor nanoparticle composites

Rupam Mukherjee, Zhi-Feng Huang, and Boris Nadgorny
Department of Physics and Astronomy, Wayne State University, Detroit, Michigan 48201, USA

(Received 5 September 2014; accepted 17 October 2014; published online 28 October 2014)

Multiple percolation transitions are observed in a binary system of RuO_2-$CaCu_3Ti_4O_{12}$ metal-semiconductor nanoparticle composites near percolation thresholds. Apart from a classical percolation transition, associated with the appearance of a continuous conductance path through RuO_2 metal oxide nanoparticles, at least two additional tunneling percolation transitions are detected in this composite system. Such behavior is consistent with the recently emerged picture of a quantum conductivity staircase, which predicts several percolation tunneling thresholds in a system with a hierarchy of local tunneling conductance, due to various degrees of proximity of adjacent conducting particles distributed in an insulating matrix. Here, we investigate a different type of percolation tunneling staircase, associated with a more complex conductive and insulating particle microstructure of two types of non-spherical constituents. As tunneling is strongly temperature dependent, we use variable temperature measurements to emphasize the hierarchical nature of consecutive tunneling transitions. The critical exponents corresponding to specific tunneling percolation thresholds are found to be nonuniversal and temperature dependent. © *2014 AIP Publishing LLC*.
[http://dx.doi.org/10.1063/1.4900777]

Percolation is one of the most fundamental and far-reaching physical phenomena, with major implications in a vast variety of fields.[1,2] The observation of a conductivity threshold in a mixture of a metallic filler in an insulating matrix is one of the simplest manifestations of a classical percolation process, which governs transport and many other properties of the system.[3] In the case of classical percolation, at the percolation threshold with filler volume fraction p_c, the geometrical connectivity is beginning to span across the entire system, leading to the appearance of an infinite cluster.[1] Consequently, near p_c, the resistivity of a composite can be expressed as $R \propto (p\text{-}p_c)^{-\mu}$. The critical exponent μ can be considered universal, i.e., material-independent, contingent only on the dimensionality of the system, provided that the local microstructure of a system is isotropic and has only short range correlations.[4] The universality of μ ($\mu \sim 2$ in 3D) can be well described by random resistor network models.[5–7] Indeed, in many experiments, this value lies within a fairly narrow range from 1.7 to 2.[1,4,8] However, in almost half of the experiments μ deviates from the universal value, often quite dramatically—sometimes exceeding it by almost an order of magnitude.[5]

This puzzling behavior has been habitually attributed to various tunneling processes between particles or random clusters.[8,9] However, at least, at first sight, percolation and tunneling phenomena are not easy to reconcile. While the definition of a threshold—as a point at which electrical conductivity vanishes—in classical percolation is straightforward, it is conceptually much more difficult to assign a threshold value in the case of tunneling. Strictly speaking, tunneling conductance between particles comprising a percolative network should always exist, albeit exponentially small at larger interparticle distances. Assuming no sharp cut-off and a random distance distribution between particles, one would generally expect variable-range tunneling mechanism to dominate the conductance across such a network, resulting in an exponential-type behavior with no distinct percolative thresholds. On the other hand, multiple percolation transitions can be envisioned in the case of lattice-like microstructure of the composite systems, with specific relationships between the particle size D, the characteristic tunneling length ξ and the interparticle distance r, in which classical percolation transition can be supplemented by a tunneling transition.[6,10–13] In order to distinguish between these cases, experimentally straightforward conductivity measurements may not suffice. For example, in earlier work, percolation behavior was studied on carbon black-resin[9,14] or ZnO-polymer[10] composite systems. Tunneling-controlled mechanism was expected due to the low percolation limits and the related slow change of resistivity measured.[10] Two distinct regions corresponding to classical and tunneling percolation transitions were identified by linking non-ohmic behavior in one of these regions to a tunneling percolation transition.[9,15,16] Recently, Wei *et al.* reported the existence of two percolation thresholds in $Ag_x(SnO_2)_{1-x}$ nanogranular films from temperature-dependent conductivity measurements.[17] Similarly, by using conductance atomic force microscopy for the Ni-SiO_2 composite system, the first order tunneling percolative behavior (in contrast to higher order ones) was established.[12] In the framework of global tunneling network (GTN), Balberg, Grimaldi, and co-workers have studied the tunneling process in some conductor-insulator composites with continuum insulating matrix.[6,13,18] Theoretically, it has been well established that in composites, the competition between percolation and tunneling behavior depends solely on the microstructure and the ratio of metallic particle size D to the tunneling length ξ.[4,6,19]

Additionally, one can envision a series of percolation thresholds due to interparticle tunneling, which has been

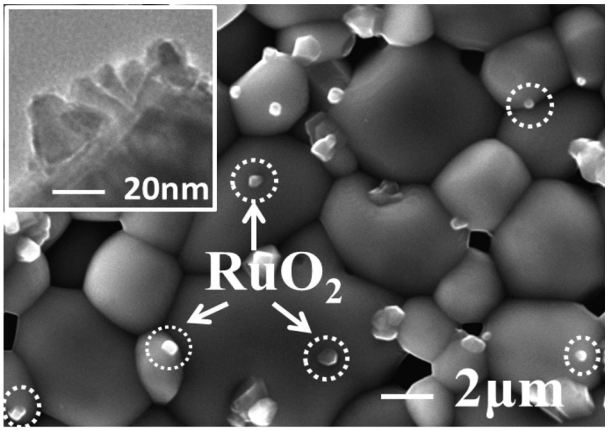

FIG. 1. SEM image of RuO_2-CCTO composite system, with RuO_2 particles indicated by dotted circles. Inset: High-resolution TEM image of grain structure in CCTO.

referred to as a tunneling staircase.[20] In order to implement a system with such properties, local resistivity between the n-th nearest neighbors, ρ_n, should be orders of magnitude higher than that between the (n-1)-th nearest neighbors, ρ_{n-1}, with ρ_n being the highest local resistivity in the system.[20] We note, however, that one can further generalize the condition for tunneling staircase to a multi-component system with different resistivity of constituents, as long as one type of resistance network dominates at a given composition.

In this letter, in addition to a classical percolation threshold resulting from the occurrence of a percolated conducting cluster across metallic oxide RuO_2 nanoparticles that are mixed with another type of particles, $CaCu_3Ti_4O_{12}$ (CCTO), we observe at least two additional tunneling percolation thresholds in a four-step tunneling staircase. Compared to most other percolation systems studied experimentally or theoretically, the nanocomposite system examined here consists of two types of non-spherical particles of different sizes. The system can then be described as a conducting (tunneling) network of one nanoparticle type (RuO_2) packed with another type of semiconducting particles (CCTO), instead of being embedded in a continuum insulating medium as in conventional percolation systems. The observation of a hierarchical nature of percolation staircase in this binary network becomes especially revealing when variable temperature conductivity measurements are utilized. We find that the critical exponents for various tunneling percolation thresholds are strongly temperature dependent, a distinguishing feature of tunneling behavior which has been missing in previous studies of percolation systems.

Samples of CCTO were prepared via solid state process, by mixing $CaCO_3$ (99.99%), CuO (99.99%), and TiO_2 (99.99%) in a planetary ball mill.[21] In the presence of acetone, the mixture was ball-milled using zirconia balls for 1 h and pre-calcined at 1000 °C for 12 h. It was then mixed with different volume fractions p of ruthenium oxide RuO_2 of 99.99% metal basic (Sigma Aldrich). Pellets of RuO_2-CCTO composites were prepared by using a cold pressed die with a uniaxial pressure of 1 GPa, and then calcined at 1100 °C prior to resistivity measurement. PPMS (Quantum Design) along with the four-point technique was used to measure the temperature dependent resistivity of the composites. Scanning Electron Microscope (SEM, JEOl, 6610LV) with an Energy Dispersive Spectroscopy (EDS) detector (Oxford) was used for compositional and morphological analysis. In a separate set of experiments, we have also prepared the host CCTO by a different (sol-gel) technique. This set of experiment yielded similar tunneling behavior also characterized by the presence of a tunneling percolation staircase. The slight differences observed in the values of percolation thresholds and critical exponents are likely to originate from somewhat different microstructure (e.g., of grains and grain boundaries) of CCTO particles.

Figure 1 shows a typical micrograph of the distribution of RuO_2 filler in a RuO_2-CCTO composite system. The grain size of CCTO is about 5–10 μm, and RuO_2 particles are around 400–500 nm. By performing a detailed EDX composition analysis, we found that substantial amount of RuO_2 has diffused into CCTO grains. Thus, while nominally our system consists of a bulk semiconducting CCTO and a metallic RuO_2 filler, the real microstructure of this system is more complicated, due to the presence of an insulating surface layer and grain boundaries of CCTO, which is likely to affect percolation tunneling staircase. Figures 2(a) and 2(b) show the variation in conductance σ with metallic volume fraction p at 300 K for RuO_2-CCTO composite systems, with the power law fitting $\sigma \propto (p\text{-}p_c)^{\mu}$ to determine the scaling behavior of different tunneling percolation stairs. Four conductivity stairs can be identified, along with three distinct percolation thresholds and the corresponding critical exponents. Thus, the definitive picture of percolation staircase with multiple percolation transitions is presented in this

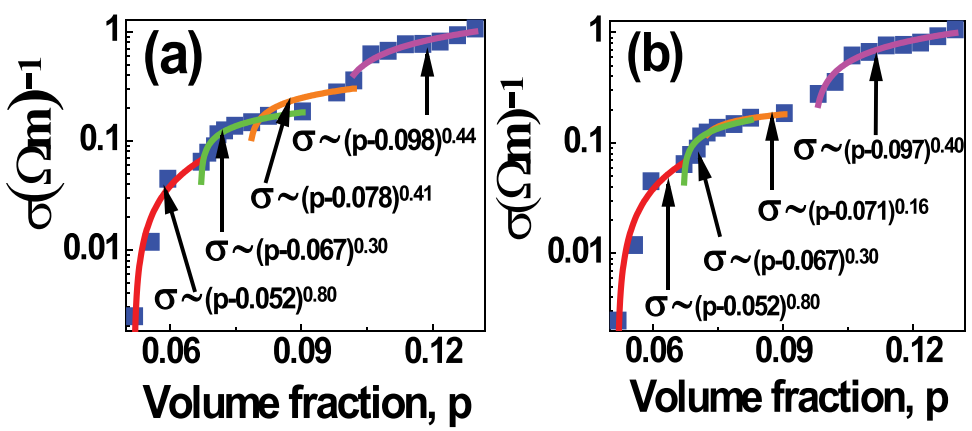

FIG. 2. System conductivity as a function of volume fraction of RuO_2, as measured at 300 K. Two sets of slightly different percolation thresholds are used in the power law fitting, including: (a) thresholds found from the resistance ratio R_{270K}/R_{300K} measurement given in Fig. 3(a); and (b) thresholds extracted from the R_{250K}/R_{300K} measurement in Fig. 3(b).

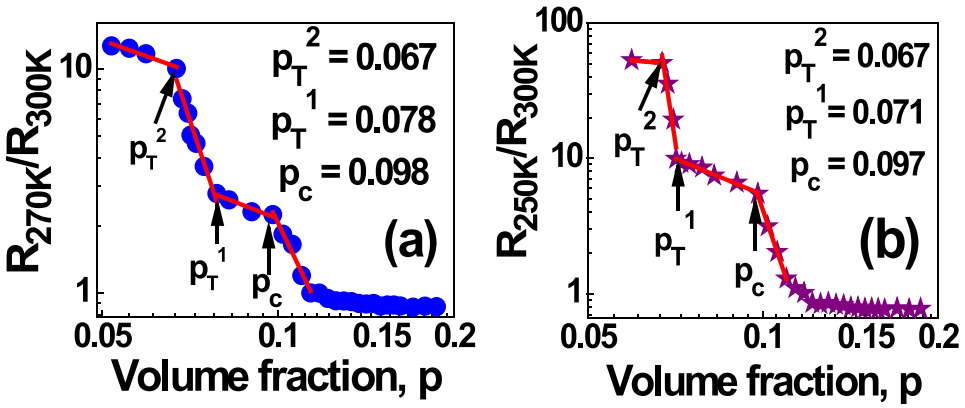

FIG. 3. Resistance ratios (a) R_{270K}/R_{300K} and (b) R_{250K}/R_{300K} as a function of volume fraction p. Three percolation thresholds, p_T^1, p_T^2 (first and second tunneling thresholds), and p_c (the classical percolation threshold), are identified from the inflection points of the power law fitting in the log-log plots.

binary particle-packing network, showing a hierarchy of tunneling conductance. We note that while our data are consistent with a tunneling staircase, the accuracy of the scaling fits should be carefully examined. Indeed, the data can be equally well fitted by using slightly different values of percolation thresholds and critical exponents, as shown in Figs. 2(a) and 2(b). To reveal a more nuanced picture of conduction and to distinguish between classical and tunneling percolation behavior, we use temperature dependent transport measurements (see Figs. 3 and 4). Since tunneling is typically strongly temperature dependent, it is sufficient in our case to lower the temperature by just 50 K below the room temperature to see a significant difference from the room temperature data. At the same time, experimentally one is normally limited by the highest measurable resistance, which sets up the low temperature limit of our measurement.

Such temperature dependent effects are illustrated in Figs. 3(a) and 3(b), which give the ratio of sample resistance

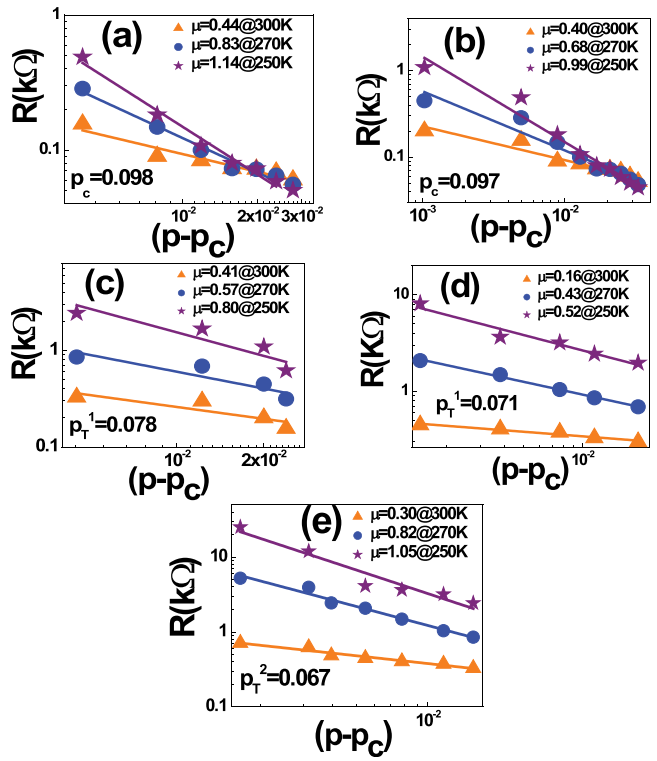

FIG. 4. Scaling behavior of the sample resistance near different percolation thresholds at temperatures 300 K, 270 K, and 250 K. Values of percolation thresholds determined in Fig. 3 are used, with the corresponding critical exponents indicated in each panel.

at a given temperature to the room-temperature resistance, i.e., R_{270K}/R_{300K} and R_{250K}/R_{300K} for the temperatures of 270 K and 250 K, respectively, as a function of volume fraction p. Three percolation thresholds, p_C, p_T^1, and p_T^2, can be clearly identified from the inflection points of the log-log plots. Note that values of these thresholds determined from two independent measurements (R_{270K}/R_{300K} vs. R_{250K}/R_{300K}) are slightly different, leading to different critical exponents as shown in Fig. 2. This can be expected from strong temperature dependence of tunneling conductance, which is pivotal for accurate determination of thresholds in systems governed by both percolation and tunneling.

An important feature given in Fig. 3 is associated with a series of sharp increases in the resistance ratios R_{270K}/R_{300K} and R_{250K}/R_{300K} when going from high to low volume fraction of RuO_2. The first increase occurs from $p \sim 0.12$ to 0.098 (0.097), the first inflection point, followed by a steep rise in the rate of resistance change. We argue that, in spite of a relatively large resistance ratio near the threshold ($R_{250K}/R_{300K} \sim 8$), this point corresponds to a classical percolation transition. Indeed, at $p \sim 0.11$, the resistance ratios approach 1, whereas the ratio R_{250K}/R_{300K} for bulk RuO_2 is approximately 0.75. This implies that some fractions of the active bonds are already tunneling bonds, which have a resistance ratio greater than one. Across the volume fraction range between 0.11 and 0.098, the number of tunneling bonds further increase at the expense of classical bonds between RuO_2 particles. This can also be viewed as the decrease in the number of effective parallel metallic resistors in the matrix. Thus, we can roughly estimate the resistance of such RuO_2 direct conductance paths by calculating the resistance of equivalent RuO_2 "nanowires," $R = 4\rho L/\pi D^2$, where $\rho = 40\ \mu\Omega\cdot$cm is the resistivity of RuO_2, $L \sim 5$–10 mm (the size of the pellet) is the length of a nanowire near the percolation threshold, and $D = 0.5\ \mu$m is the average diameter of RuO_2 particles. This results in the resistance of approximately 1–10 kΩ for a few "nanowires" connected in parallel. On the other hand, the resistance measured at the threshold $p = 0.098$ is around 100 Ω, at least an order of magnitude smaller, indicating that the temperature dependent contribution is largely due to the tunneling conductance. Our conclusion that $p = 0.098$ (0.097) corresponds to the classical percolation threshold is in agreement with earlier measurement of the dielectric permittivity in this composite system, which also shows a peak at $p \sim 0.10$.[22]

On the other hand, another two thresholds observed at $p < 0.098$ correspond to tunneling percolation. In contrast to most other systems showing percolation staircase as a result of tunneling between non-contacted conducting particles of various degree of nearest neighbors,[12,16,19] the binary network studied here corresponds to much more complicated tunneling processes, facilitated by surface oxide layers and interior grain boundaries of CCTO. This is further complicated by partial diffusion of Ru into CCTO grains, leading to the complex tunneling percolation effects observed in this system. To examine the origin of these effects, we have taken high resolution TEM images to determine the microscopic structure of CCTO (see the inset in Fig. 1). We observe nanometer-size grain boundaries, which are within the range required for tunneling processes. Once we identified features of the appropriate size, we can speculate about the hierarchy of the corresponding tunneling processes. The lowest threshold, p_T^2, is likely to correspond to bulk tunneling across the CCTO matrix, as—below this point—the resistance is practically independent of RuO_2 concentration. On the other hand, above p_T^2, RuO_2 interparticle tunneling across CCTO grain boundaries may take place, while above p_T^1, tunneling may be further assisted by continuous Ru doping of CCTO surface layers and grain boundaries, as seen from the elemental analysis. Further detailed studies of the composites microstructure are needed to solidify these assumptions.

The scaling behavior of the staircase (i.e., near various percolation thresholds for the hierarchy of stairs) at 3 different temperatures and the corresponding critical exponents μ are given in Figs. 4(a)–4(e), with percolation thresholds determined from ratios of R_{270K}/R_{300K} and R_{250K}/R_{300K} as described above. For all the percolation stairs, values of the critical exponent for this binary particle network are found to decrease with the increase of temperature, and substantially vary for different thresholds of the tunneling staircase. In addition, for this RuO_2-CCTO composite, the critical exponents show a significant deviation from universal values which typically range from 1.7 to 2. We note that, while such nonuniversality of critical exponents—particularly the dependence on p_c and the material type—has been verified experimentally in tunneling percolation[5,17,23] and explained theoretically,[5,24] temperature dependent critical exponents have not been observed before.

In summary, we have studied the multiple percolation behavior in a RuO_2-CCTO composite system. In contrast to previously studied percolation systems with continuum insulating medium, this system has a complex microstructure and consists of two particle types of large size and conductivity disparity. In addition to a classical percolation threshold, we identify two separate tunneling thresholds based on temperature dependence of tunneling conductance, as well as a hierarchy of four conductivity stairs, supporting the theoretical notion of tunneling staircase in the case of complex microscopic structure of a composite system. The nonuniversality of the scaling behavior in tunneling percolation is examined by temperature dependent transport measurements, showing not only large variations of critical exponent values, deviating from the universal range for different percolation thresholds and tunneling stairs, but also the new temperature effect on critical exponents. Our study further demonstrates that detailed microstructures and the complexity of multi-component composite systems play a key role in revealing various new phenomena in percolative networks that control system properties and functionalities.

This work was supported by the National Science Foundation under Grants ECCS-0923292, DMR-1006381 (B.N.) and DMR-0845264 (Z.-F. H.).

[1]D. Stauffer and A. Aharony, *Introduction To Percolation Theory* (Taylor & Francis, 1994).
[2]A. Hunt and R. Ewing, *Percolation Theory for Flow in Porous Media* (Springer, 2009).
[3]M Sahini and M Sahimi, *Applications of Percolation Theory* (CRC Press, 1994).
[4]S.-I. Lee, Y. Song, T. W. Noh, X.-D. Chen, and J. R. Gaines, Phys. Rev. B **34**(10), 6719 (1986).
[5]S.-V. Menot, C. Grimaldi, T. Maeder, S. Strässler, and P. Ryser, Phys. Rev. B **71**(6), 064201 (2005).
[6]G. Ambrosetti, C. Grimaldi, I. Balberg, T. Maeder, A. Danani, and P. Ryser, Phys. Rev. B **81**(15), 155434 (2010).
[7]B. Derrida, D. Stauffer, H. J. Herrmann, and J. Vannimenus, J. Phys. Lett. **44**(17), 701 (1983).
[8]A. Celzard, E. McRae, J. F. Marêché, G. Furdin, M. Dufort, and C. Deleuze, J. Phys. Chem. Solids **57**(6–8), 715 (1996).
[9]S. Nakamura, K. Saito, G. Sawa, and K. Kitagawa, Jpn. J. Appl. Phys. Part 1 **36**(8), 5163 (1997).
[10]J. I. Hong, L. S. Schadler, R. W. Siegel, and E Mårtensson, Appl. Phys. Lett. **82**(12), 1956 (2003).
[11]I. Balberg, J. Phys. D: Appl. Phys. **42**(6), 064003 (2009).
[12]D. Toker, D. Azulay, N. Shimoni, I. Balberg, and O. Millo, Phys. Rev. B **68**(4), 041403 (2003).
[13]G. Ambrosetti, I. Balberg, and C. Grimaldi, Phys. Rev. B **82**(13), 134201 (2010).
[14]J. B. Donnet, R. C. Bansal, and M. J. Wang, *Carbon Black* (Science and Technology, New York, 1993), p. 62.
[15]Y. Fujikura, Polym. J. **21**(8), 609 (1989).
[16]E. K. Sichel, J. I. Gittleman, and Ping Sheng, Phys. Rev. B **18**(10), 5712 (1978).
[17]Y.-F. Wei and Z.-Q. Li, Appl. Phys. Lett. **102**(13), 131911 (2013).
[18]I. Balberg, Phys. Rev. Lett. **59**(12), 1305 (1987).
[19]N. Johner, C. Grimaldi, I. Balberg, and P. Ryser, Phys. Rev. B **77**(17), 174204 (2008).
[20]I. Balberg, D. Azulay, Y. Goldstein, J. Jedrzejewski, G. Ravid, and E. Savir, Eur. Phys. J. B **86**, 428 (2013).
[21]H. Yu, H. Liu, H. Hao, L. Guo, C. Jin, Z. Yu, and M. Cao, Appl. Phys. Lett. **91**(22), 222911 (2007).
[22]R. Mukherjee, G. Lawes, and B. Nadgorny, Appl. Phys. Lett. **105**(7), 072901 (2014).
[23]Z. Rubin, S. A. Sunshine, M. B. Heaney, I. Bloom, and I. Balberg, Phys. Rev. B **59**(19), 12196 (1999).
[24]C. Grimaldi and I. Balberg, Phys. Rev. Lett. **96**(6), 066602 (2006).